International Journal of Nanomedicine

Dovepress
open access to scientific and medical research

Open Access Full Text Article

ORIGINAL RESEARCH

Nanofunctionalized zirconia and barium sulfate particles as bone cement additives

This article was published in the following Dove Press journal:
International Journal of Nanomedicine
15 December 2009
Number of times this article has been viewed

Riaz Gillani[1]
Batur Ercan[1]
Alex Qiao[3]
Thomas J Webster[1,2]

[1]Division of Engineering, [2]Department of Orthopaedics, Brown University, Providence, RI, USA; [3]G3 Technology Innovations, LLC, Pittsford, NY, USA

Abstract: Zirconia (ZrO_2) and barium sulfate ($BaSO_4$) particles were introduced into a methyl methacrylate monomer (MMA) solution with polymethyl methacrylate (PMMA) beads during polymerization to develop the following novel bone cements: bone cements with unfunctionalized ZrO_2 micron particles, bone cements with unfunctionalized ZrO_2 nanoparticles, bone cements with ZrO_2 nanoparticles functionalized with 3-(trimethoxysilyl)propyl methacrylate (TMS), bone cements with unfunctionalized $BaSO_4$ micron particles, bone cements with unfunctionalized $BaSO_4$ nanoparticles, and bone cements with $BaSO_4$ nanoparticles functionalized with TMS. Results demonstrated that *in vitro* osteoblast (bone-forming cell) densities were greater on bone cements containing $BaSO_4$ ceramic particles after four hours compared to control unmodified bone cements. Osteoblast densities were also greater on bone cements containing all of the ceramic particles after 24 hours compared to unmodified bone cements, particularly those bone cements containing nanofunctionalized ceramic particles. Bone cements containing ceramic particles demonstrated significantly altered mechanical properties; specifically, under tensile loading, plain bone cements and bone cements containing unfunctionalized ceramic particles exhibited brittle failure modes whereas bone cements containing nanofunctionalized ceramic particles exhibited plastic failure modes. Finally, all bone cements containing ceramic particles possessed greater radio-opacity than unmodified bone cements. In summary, the results of this study demonstrated a positive impact on the properties of traditional bone cements for orthopedic applications with the addition of unfunctionalized and TMS functionalized ceramic nanoparticles.

Keywords: orthopedic, nanotechnology, bone cements, osteoblasts

Introduction

Polymethyl methacrylate (PMMA) bone cement is frequently used in the fixation of orthopedic implants. While it is widely accepted that PMMA has satisfactory biocompatibility properties that warrant its use in orthopedics, PMMA is notorious for eliciting an autoimmune response that may manifest in fibrous encapsulation or inflammation, both of which contribute to possible subsequent implant loosening and failure.[1,2] This implant failure is often exacerbated by wear debris generated from brittle bone cement use, a direct product of dynamic mechanical forces acting on PMMA *in vivo*. PMMA is known to fail *in vivo*, being cited as the weakest portion of the joint–implant system.[3,4] Perhaps contributing to its suboptimal cytocompatibility properties, PMMA is known to be highly exothermic during polymerization, often leading to tissue necrosis during initial placement at the joint–implant interface.[5] In particular, Boner and colleagues have reported a high risk of tissue necrosis

Correspondence: Thomas J Webster
Division of Engineering and Department of Orthopaedics, Brown University, 184 Hope Street, Providence, RI, 02912, USA
Tel +1 401 863 2318
Fax +1 401 863 9107
Email thomas_webster@brown.edu

anytime the thickness of PMMA exceeds 5.0 mm around the implant.[6]

While there have been many attempts to improve properties of bone cements, few have employed nanotechnology (or the use of materials with one dimension less than 100 nm). Along this line, ceramic particles, such as zirconia (ZrO_2) and barium sulfate ($BaSO_4$), are often introduced into bone cements to increase radio-opacity so that they may be visualized through X-ray imaging.[7] The introduction of ceramics into bone cements has been shown by Sabokbar and colleagues to further negatively impact PMMA biocompatibility properties, often manifesting in the loosening of implants.[3] Due to many studies which have demonstrated greater bone formation on implants with nanometer surface features, it is clear that changing the properties (such as particle size and even chemistry) of such ceramics added to bone cements may improve PMMA efficacy. Previous studies have shown that material (such as metals, ceramics, polymers, and composites thereof) modifications at the nanoscale, particularly texture and topographical modifications, increase surface wettability and in turn increase cytocompatibility properties.[8]

Another approach that may be taken in conjunction with nanoscale modification of ceramic particles added to bone cements is chemical functionalization of ceramic nanoparticles to allow for better integration with PMMA. Chemical functionalization of nanoparticles may also aid in cytocompatibility properties. For example, in previous studies, polar, nucleophilic groups have been shown to increase surface energy and wettability of implant surfaces allowing for the adsorption of select proteins, such as fibronectin and vitronectin, to promote osteoblast (bone-forming cell) adhesion and proliferation.[9]

In this study, for the first time, bone cements were modified by adding unfunctionalized and functionalized ZrO_2 and $BaSO_4$ particles. Specifically, some ceramic nanoparticles were left unfunctionalized while some were functionalized with a silane-coupling agent 3-(trimethoxysilyl)propyl methacrylate (TMS). Bone cements were further seeded with osteoblasts and incubated for four and 24 hours. Scanning electron microscopy (SEM) imaging was used to examine ceramic particle dispersion in the bone cements to determine the relationship between particle dispersion and observed cell densities. Tensile and compressive tests were also carried out to characterize differences in stress–strain properties. SEM imaging was used to further characterize the mechanical failure modes of the bone cements in response to tensile loading. Exothermic testing was conducted on bone cements during polymerization in order to determine the impact of ceramic particles on PMMA heat generation. Finally, X-ray images of the bone cements were taken to determine how the novel ceramic particles influenced radio-opacity. Results provided much promise for the use of functionalized nanoceramic particles added to PMMA for orthopedic applications.

Materials and methods

Materials

Bone cements used in the cytocompatibility testing consisted of a 5:1 ratio of liquid methyl methacrylate monomer to polymethyl methacrylate (PMMA) beads (MMA, 80-62-6; Polysciences, Inc., Warrington, PA, USA). Ten grams of liquid MMA were combined with 2 g of PMMA. Aside from the control unmodified bone cement samples, all samples contained an additional 1 g of one of the following ceramics: ZrO_2 micron particles (1314-23-4; Sigma-Aldrich, St. Louis, MO, USA), unfunctionalized ZrO_2 nanoparticles (NN-Labs, Fayetteville, AR, USA), ZrO_2 nanoparticles functionalized with TMS (NN-Labs), $BaSO_4$ micron particles (1142ZJ, NanoAmor, Houston, TX, USA), unfunctionalized $BaSO_4$ nanoparticles (1141ZJ, NanoAmor), or $BaSO_4$ nanoparticles functionalized with TMS (NN-Labs). Bone cements were made by adding PMMA beads into liquid MMA. The reaction was catalyzed with 1,1'-Azobis(cyclo-hexanecarbonitrile) (0.05% by mass of liquid MMA). After the addition of the catalyst, the PMMA-MMA mixtures were stirred vigorously in a 70 °C hot water bath. For bone cements containing ceramic particles, the ceramic particles were stirred into the mixture for a total of five minutes until reaching a viscous consistency. Then, they were cast into polystyrene petri dishes, in which they were allowed to cool for a period of 48 hours. After setting, the bone cements were sectioned into approximately 1 cm^2 substrates for cytocompatibility testing.

Cytocompatibility testing

The samples were soaked in 70% ethyl alcohol for sterilization purposes for approximately 10 minutes and subsequently seeded at a density of 3500 cells/cm^2 with human osteoblasts (population numbers 6 to 12, American Type Culture Collection CEL-11372) in osteoblast cell culture medium (Dulbecco's modified Eagle medium [DMEM]) supplemented with 10% fetal bovine serum (FBS) and 1% P/S. Prior to the experiment, osteoblasts were cultured in osteoblast cell culture medium under standard culture conditions (5% CO_2/95% air at 37 °C). Cell-seeded

samples were incubated at 37 °C for either four or 24 hours under standard cell culture conditions.

After incubation, samples were rinsed with phosphate-buffered saline (PBS) to remove nonadherent cells, and were subsequently fixed in 10% formaldehyde for 10 minutes. Then, samples were stained with 1% DAPI fluorescent dye (Sigma Aldrich) for 10 minutes. Cells were visualized using a fluorescence microscope (Leica DM 5500B; Leica, Austin, TX, USA) and cell densities were counted on five randomly selected sites on each sample. Experiments were conducted in duplicate and repeated at least three times.

Tensile and compressive mechanical testing

Bone cements used for mechanical testing were prepared using a protocol similar to that which was just described. The protocol only differed in the ratio of MMA to PMMA used in each sample: instead of a 5:1 ratio, a 1:1 ratio was used to fabricate bone cements that would solidify more quickly and allow for better dispersion of ceramic particles. In the preparation of each sample, 12 g of MMA were combined with 12 g of PMMA, while 2 g of one of the six ceramic particles (ZrO_2 micron particles, unfunctionalized ZrO_2 nanoparticles, ZrO_2 nanoparticles functionalized with TMS, $BaSO_4$ micron particles, unfunctionalized $BaSO_4$ nanoparticles, and $BaSO_4$ nanoparticles functionalized with TMS) were added to the modified bone cements. The PMMA beads and ceramic particles were first introduced into a 50 mL beaker to a 70 °C water bath. Subsequently, the liquid phase of MMA with the dissolved 1,1'-Azobis(cyclo-hexanecarbonitrile) catalyst was poured onto the solid phase and the resulting mixture was stirred vigorously and poured into a 250 mm × 25 mm × 2.5 mm Teflon mold. Bone cements were allowed to harden at room temperature for a period of 3–7 days, after which they were excised from the molds. A fine-tooth saw and vice were used to partition the larger samples into smaller rectangular samples for tensile and compressive mechanical testing. For tensile testing, specimens of dimensions 24.3 mm × 59.5 mm × 1.8 mm were excised. For compressive testing, specimens of dimensions 24.3 mm × 10.3 mm × 1.8 mm were excised.

Specimens were tested for their tensile and compressive properties using 500 N and 100 kN load cells (Instron 5800 Electro-Mechanical Testing System; Instron Pty Ltd., Melbourne, Australia). Tensile specimens were clamped and extended at a rate of 2 mm/minute until failure. Compressive specimens were allowed to rest on a flat platform and were compressed 1 mm at a rate of 0.2 mm/minute. Due to geometrical constraints, compressive specimens were not compressed until failure. Cross-sectional force (1.8 mm × 24.3 mm for tensile specimens and 10.3 mm × 1.8 mm for compressive specimens) was measured consistently throughout extension and compression and stress-strain curves were developed for each of the samples. Three trials were averaged for all bone cements.

Scanning electron microscopy

Using a LEO 1530VP SEM, the bone cements used in the cytocompatibility tests were characterized for ceramic particle dispersion and topography prior to testing. Additionally, bone cements used in the tensile tests were characterized for their mode of fracture. Samples were prepared for SEM by sputter-coating with gold and palladium for one minute.

Temperature measurements of bone cements during polymerization

To evaluate differences in exothermic properties, 0.75 g of MMA with the catalyst was poured into a glass test tube containing 0.75 g of PMMA beads as well as 0.25 g of the ceramic particles aside from the plain sample, in which no ceramic particles were added. The contents of the glass test tube were stirred vigorously in a 70 °C hot water bath until a temperature threshold of 60 °C was reached. At this time, the test tube was removed from the water bath and the temperature of the polymerizing bone cements was measured periodically over ten minutes using a Fluke 50 Series II contact thermometer (Fluke Electronics, Everett, WA, USA).

X-ray analysis of radio-opacity

Samples used in tensile and compressive testing were visualized for radio-opacity using a Bennett X-ray Technologies Model S-82RM (Bennett X-Ray Technologies, Copiague, NY, USA) machine. The resulting X-ray image was scanned using a HPColor Laserjet CM1015 scanner (Hewlett-Packard, Houston, TX, USA) for analysis of mean grey values (a measure of optical density) using ImageJ 1.41 software (National Institutes of Health, Bethseda, MD, USA).

Statistical analyses

Numerical data was analyzed using Microsoft Excel (Microsoft Corp., Redmond, WA, USA). One-tailed, heteroscedastic *t*-tests were used to analyze significant differences between bone cements in cytocompatibility testing.

Results

Scanning electron microscopy

Differences in ceramic particulate dispersion patterns could be clearly seen in the various bone cements formulated here (Figure 1). It appeared that micron particles were not as readily visible on the surface as they were immersed below the surface due to sedimentation. In contrast, functionalized nanoparticles could be easily seen on the surfaces of the bone cements. Bone cements containing functionalized ZrO_2 nanoparticles tended to aggregate more than their unfunctionalized counterparts.

Cytocompatibility testing

After four hours, osteoblast cell density assays demonstrated greater osteoblast adhesion on bone cements containing $BaSO_4$ particles ($P < 0.05$ for micron, $P < 0.05$ for nanounfunctionalized, and $P < 0.005$ for nanofunctionalized with TMS) compared to unmodified bone cements (Figure 2). The average cell densities (cells/cm^2) for each type of bone cement, plus or minus one standard error, were as follows: unmodified bone cements (Plain): 298 ± 31.4, bone cements with $BaSO_4$ micron particles (BM): 372.6 ± 36.9, bone cements with unfunctionalized $BaSO_4$ nanoparticles (BN): 394 ± 49.2, bone cements with $BaSO_4$ nanoparticles functionalized with TMS (BNFT): 429 ± 43.5, bone cements with ZrO_2 micron particles (ZM): 254 ± 44.6, bone cements with unfunctionalized ZrO_2 nano particles (ZN): 288 ± 39.4, and bone cements with ZrO_2 nanoparticles functionalized with TMS (ZNFT): 282 ± 32.2.

After 24 hours, results demonstrated greater osteoblast density on all bone cements containing ceramic particles ($P < 0.1$ for $BaSO_4$ micron particles, $P < 0.005$ for unfunctionalized $BaSO_4$ nanoparticles and ZrO_2 nanoparticles functionalized with TMS, and $P < 0.001$ for $BaSO_4$ nanoparticles functionalized with TMS, ZrO_2 micron particles, and unfunctionalized ZrO_2 nanoparticles) compared to unmodified bone cements (Figure 3). Additionally, compared to bone cements containing $BaSO_4$ micron particles, osteoblast density was found to be greater on bone cements containing functionalized $BaSO_4$ nanoparticles ($P < 0.1$). Finally, compared to bone cements containing ZrO_2 micron particles, osteoblast density was greater on bone cements containing ZrO_2 nanoparticles, both unfunctionalized ($P < 0.05$) and functionalized with TMS ($P < 0.1$). The average cell densities (cells/cm^2) for each type of bone cement, plus or minus one standard error, were as follows: unmodified bone cements (Plain): 869 ± 138.4, bone cements with $BaSO_4$ micron particles (BM): 1098 ± 138.1, bone cements with unfunctionalized $BaSO_4$ nanoparticles (BN): 1335 ± 152.2, bone cements with $BaSO_4$ nanoparticles functionalized with TMS (BNFT): 1545 ± 167, bone cements with micron ZrO_2 particles (ZM): 1440 ± 144.3, bone cements with unfunctionalized ZrO_2 nanoparticles (ZN): 2104 ± 257.2, and bone cements with ZrO_2 nanoparticles functionalized with TMS (ZNFT): 2039 ± 353.

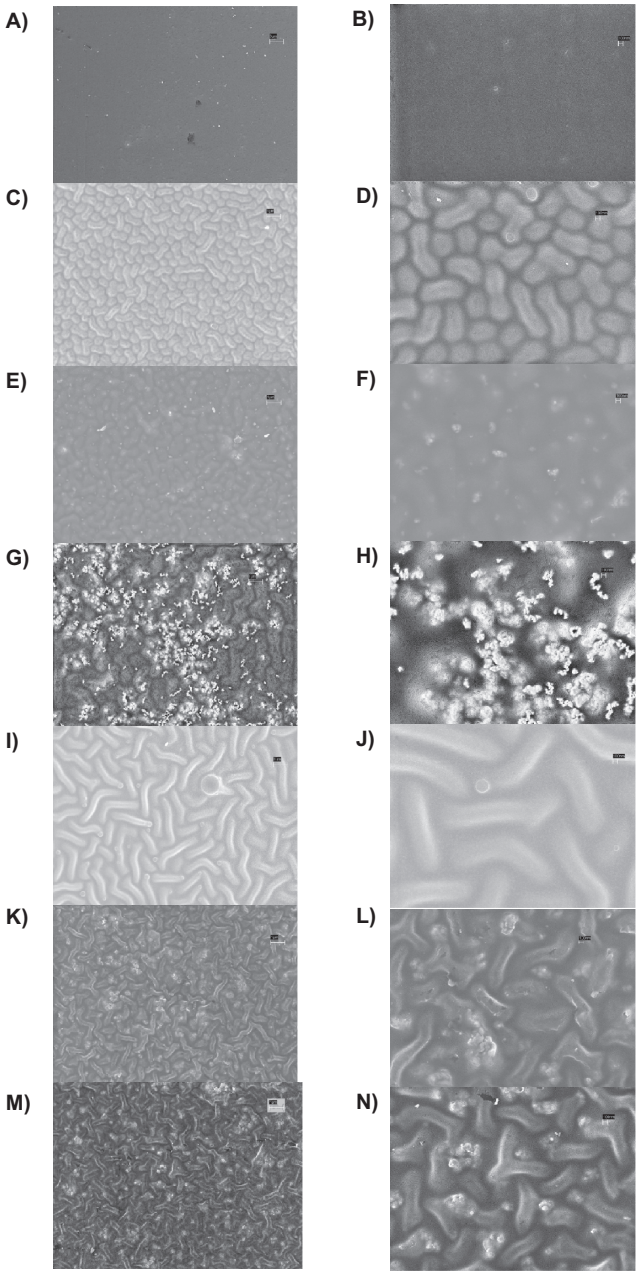

Figure 1 SEM images of bone cements used in cytocompatibility testing [Left: 15K X (scale bar = 1 μm), Right: 50K X (scale bar = 100 nm)]: Plain (**A, B**), ZM (containing micron particulate ZrO_2) (**C, D**), ZN (containing unfunctionalized ZrO_2 nano-particles) (**E, F**), ZNFT (containing functionalized ZrO_2 nano-particles) (**G, H**), BM (containing micron particulate $BaSO_4$) (**I, J**), BN (containing unfunctionalized $BaSO_4$ nano-particles) (**K, L**), and BNFT (containing functionalized $BaSO_4$ nano-particles) (**M, N**).

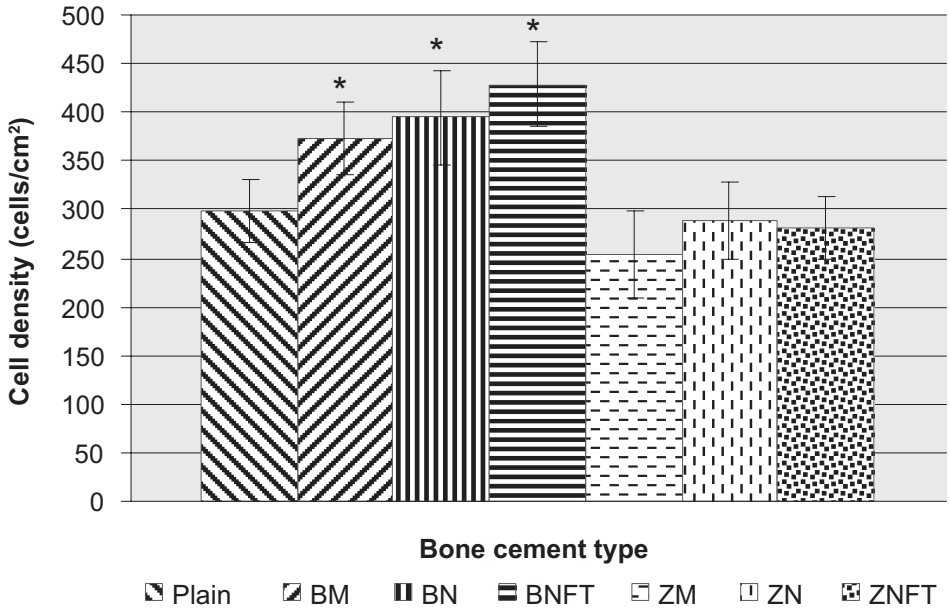

Figure 2 Osteoblast cell density, after 4 hours, as a function of bone cement type. Data = mean +/– SEM; N = 3. Plain = Unmodified bone cements; BM = Bone cements with micron particulate $BaSO_4$, BN = Bone cements with unfunctionalized $BaSO_4$ nanoparticles, BNFT = Bone cements with functionalized $BaSO_4$ nanoparticles; ZM = Bone cements with micron particulate ZrO_2, ZN = Bone cements with unfunctionalized ZrO_2 nanoparticles; ZNFT = Bone cements with functionalized ZrO_2 nanoparticles.
*Compared to plain bone cement; adhesion on bone cements containing the following ceramic particles was found to be greater: micron particulate $BaSO_4$ ($p < 0.05$), unfunctionalized $BaSO_4$ nano-particles ($p < 0.05$), and $BaSO_4$ nano-particles functionalized with TMS ($p < 0.005$).

Fluorescence microscopy images of osteoblasts after the four- and 24-hour incubation periods, respectively, further demonstrated such trends (Figures 4 and 5). Lastly, the addition of ceramic particles and their subsequent nanoscaling and chemical functionalization with the silane-coupling agent TMS, was shown to have a positive impact on osteoblast densities.

Tensile and compressive mechanical testing

Most importantly, the results of this study showed a clear difference between the failure modes for the various bone cements fabricated in this study (Figures 6 and 7). Plain bone cements as well as bone cements containing unfunctionalized ceramic micron and nanoparticles had

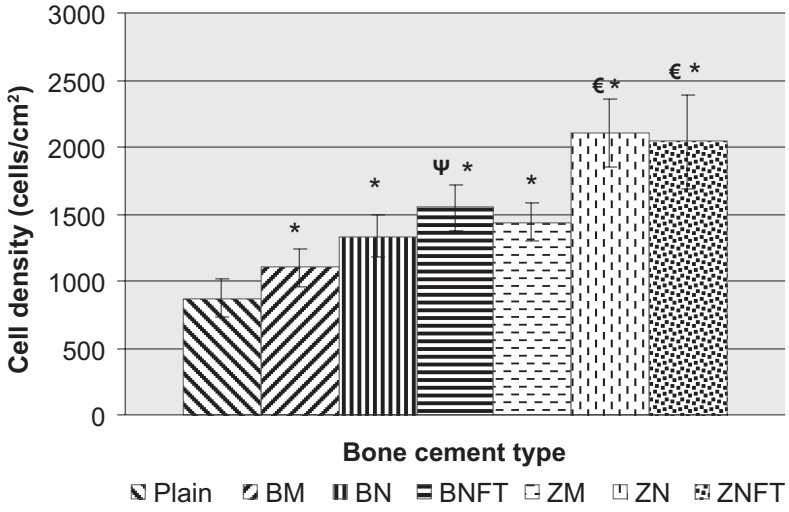

Figure 3 Osteoblast cell-density, after 24 hours, as a function of bone cement type. Data = mean +/– SEM; N = 3. Plain = Unmodified bone cements, BM = Bone cements with micron particulate $BaSO_4$, BN = Bone cements with unfunctionalized $BaSO_4$ nanoparticles, BNFT = Bone cements with functionalized $BaSO_4$ nanoparticles, ZM = Bone cements with micron particulate ZrO_2, ZN = Bone cements with unfunctionalized ZrO_2 nanoparticles, ZNFT = Bone cements with functionalized ZrO_2 nanoparticles. *Compared to plain bone cement, adhesion on bone cements containing all ceramic particles was found to be greater: micron particulate $BaSO_4$ ($p < 0.1$), unfunctionalized $BaSO_4$ nano-particles ($p < 0.005$), ZrO_2 nano-particles functionalized with TMS ($p < 0.005$), $BaSO_4$ nano-particles functionalized with TMS ($p < 0.001$), micron ZrO_2 particles ($p < 0.001$), and unfunctionalized ZrO_2 nano-particles ($p < 0.001$). $^{\Psi}$Compared to bone cements containing micron $BaSO_4$ particles, adhesion was found to be greater on bone cements containing $BaSO_4$ nano-particles functionalized with TMS ($p < 0.05$). $^{€}$WRT bone cements containing micron ZrO_2 particles, adhesion was found to be greater on bone cements containing unfunctionalized ZrO_2 nano-particles ($p < 0.05$) and ZrO_2 nano-particles functionalized with TMS ($p < 0.1$).

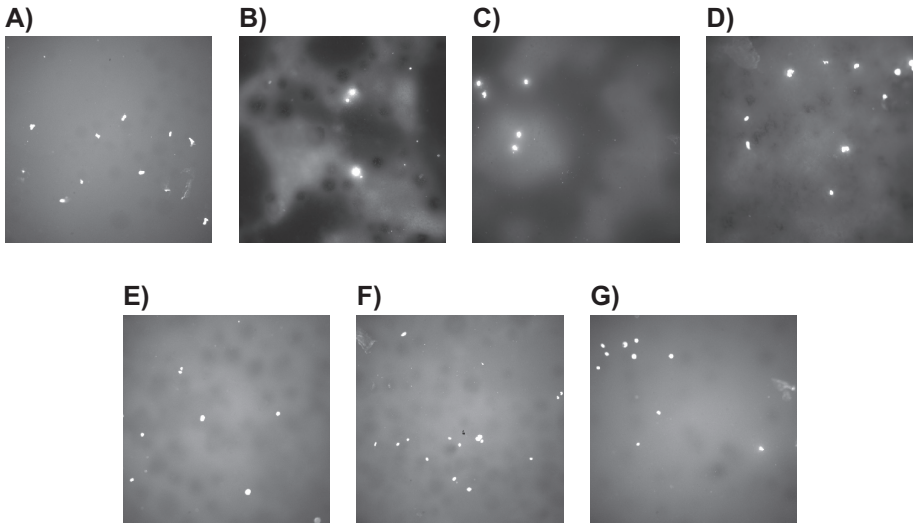

Figure 4 Fluorescence microscopy images (magnification = 10X) of osteoblasts after 4 hours of adhesion on different bone cements: **A**) Plain, **B**) ZM (containing micron particulate ZrO_2), **C**) ZN (containing unfunctionalized ZrO_2 nano-particles), **D**) ZNFT (containing ZrO_2 nano-particles functionalized with TMS, **E**) BM (containing micron particulate $BaSO_4$), **F**) BN (containing unfunctionalized $BaSO_4$ nano-additives), and **G**) BNFT (containing $BaSO_4$ nano-additives functionalized with TMS).

failure modes characteristic of brittle fracture, while bone cements containing functionalized ceramic nanoparticles had failure modes that were less brittle and had a clear plastic deformation region.

From the stress–strain data, the Young's modulus and the maximum stress under tensile loading conditions were calculated for all bone cements. This data, along with the Young's moduli of cortical and trabecular bone, are presented in Table 1 and Figures 6 and 7.[10] The maximum stress for each type of bone cement was: unmodified bone cements (Plain): 1.30E + 07 N/m^2, bone cements with $BaSO_4$ micron particles (BM): 1.25E + 07 N/m^2, bone cements with unfunctionalized $BaSO_4$ nanoparticles (BN): 1.00E+07 N/m^2, bone cements with $BaSO_4$ nanoparticles

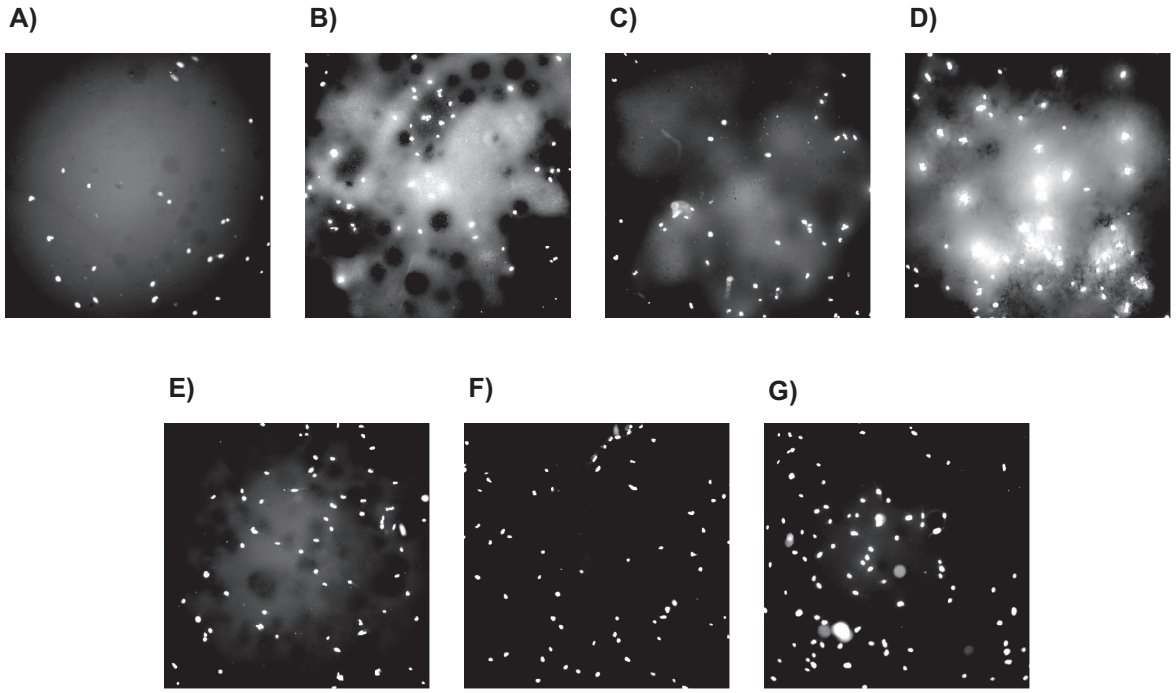

Figure 5 Fluorescence microscopy images (magnification = 10X) of osteoblasts after 24 hours of proliferation on different bone cements: **A**) Plain, **B**) ZM (containing micron particulate ZrO_2), **C**) ZN (containing unfunctionalized ZrO_2 nano-particles), **D**) ZNFT (containing ZrO_2 nano-particles functionalized with TMS, **E**) BM (containing micron particulate $BaSO_4$), **F**) BN (containing unfunctionalized $BaSO_4$ nano-additives), and **G**) BNFT (containing $BaSO_4$ nano-additives functionalized with TMS).

Table 1 Maximum stresses and Young's moduli of various bone cements under tension: Plain, ZM (containing micron particulate ZrO_2), ZN (containing unfunctionalized ZrO_2 nano-particles), ZNFT (containing functionalized ZrO_2 nano-particles), BM (containing micron particulate $BaSO_4$), BN (containing unfunctionalized $BaSO_4$ nano-particles), and BNFT (containing functionalized $BaSO_4$ nano-particles). Young's moduli values for bone obtained from study by Mente et al

Substrate	Maximum stress (N/m^2)	Young's modulus (N/m^2)
Plain	1.30E + 07	6.74E + 08
ZNFT	9.88E + 06	1.89E + 08
ZN	9.32E + 06	3.16E + 08
ZM	1.28E + 07	2.77E + 08
BNFT	1.16E + 07	2.55E + 08
BN	1.00E + 07	2.38E + 08
BM	1.25E + 07	2.98E + 08
Cortical bone – dry		1.82E + 10
Cortical bone – wet		1.24E + 10
Trabecular bone – dry		7.80E + 09

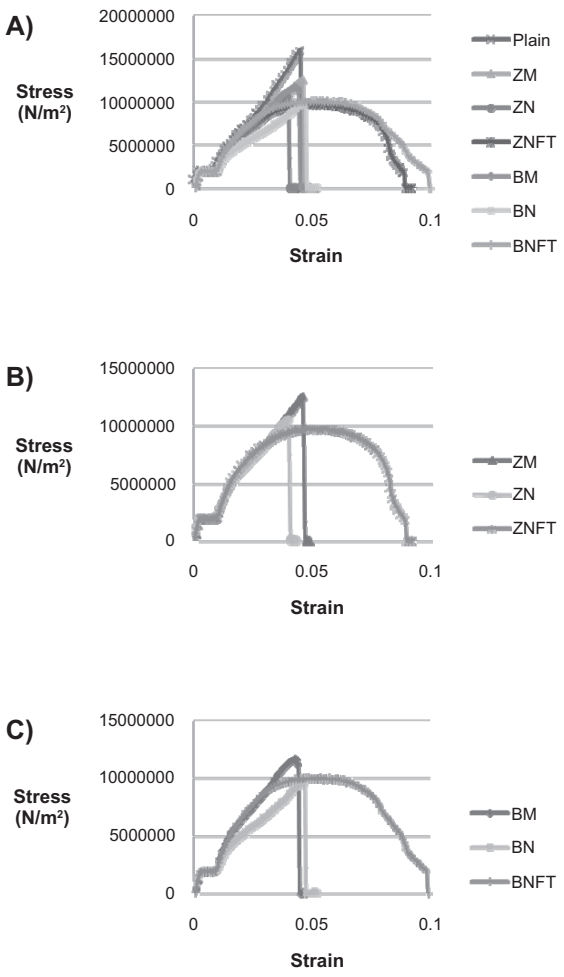

Figure 6 Representative tensile stress-strain curves for various bone cements. One representative of three trials is shown for each bone cement. Bone cements tested included: Plain, ZM (containing micron particulate ZrO_2), ZN (containing unfunctionalized ZrO_2 nano-particles), ZNFT (containing functionalized ZrO_2 nano-particles), BM (containing micron particulate $BaSO_4$), BN (containing unfunctionalized $BaSO_4$ nano-particles), and BNFT (containing functionalized $BaSO_4$ nano-particles). **A**) All bone cements, **B**) Bone cements containing ZrO_2 particles, and **C**) Bone cements containing $BaSO_4$ particles.

functionalized with TMS (BNFT): 1.16E + 07 N/m^2, bone cements with ZrO_2 micron particles (ZM): 1.28E + 07 N/m^2, bone cements with unfunctionalized ZrO_2 nanoparticles (ZN): 9.32E + 06 N/m^2, and bone cements with ZrO_2 nanoparticles functionalized with TMS (ZNFT): 9.88E + 06 N/m^2. The Young's modulus for each type of bone cement was found as follows: unmodified bone cements (Plain): 6.74E + 08 N/m^2, bone cements with $BaSO_4$ micron particles (BM): 2.98E + 08 N/m^2, bone cements with unfunctionalized $BaSO_4$ nanoparticles (BN): 2.38E + 08 N/m^2, bone cements with $BaSO_4$ nanoparticles functionalized with TMS (BNFT): 2.55E + 08 N/m^2, bone cements with ZrO_2 micron particles (ZM): 2.77E + 08 N/m^2, bone cements with unfunctionalized ZrO_2 nanoparticles (ZN): 3.16E + 08 N/m^2, and bone cements with ZrO_2 nanoparticles functionalized with TMS (ZNFT): 1.89E + 08 N/m^2.

After tensile testing, SEM was used to characterize the fractured planes in the bone cements (Figure 8). Results strongly support the suggested failure modes as observed during tensile testing. It was apparent that for bone cements undergoing brittle fracture, plain bone cements as well as bone cements with unfunctionalized ceramic micron and nanoparticles, there was clean separation of the polymer matrix from itself, as well as from the dispersed ceramic particles; this was observed particularly well in bone cements containing micron ZrO_2 particles. In bone cements with ceramic nanoparticles, while the polymer separation from the ceramic particles wasn't as readily apparent, jagged and complete fracture lines indicative of a brittle failure mode were easily observed. For bone cements containing functionalized ceramic nanoparticles, plastic failure was observed by the incomplete separation within the polymer matrix, as well as a better integration of ceramic particles into the polymer matrix.

Because compressive testing was not carried out to failure, the most meaningful data that could be derived from the stress–strain curves was the stress required to achieve a maximum strain of 56% (occurring at 1 mm of compression) (Table 2). The maximum compressive stress for each type of bone cement was: unmodified bone cements (Plain): 3.63E + 07 N/m^2, bone cements with $BaSO_4$ micron particles

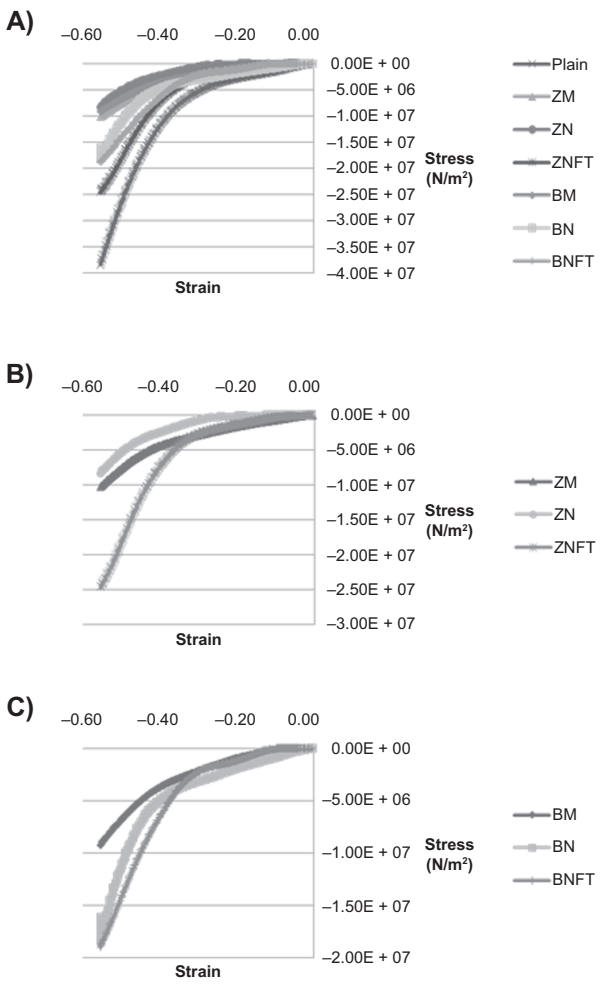

Figure 7 Representative compressive stress-strain curves for various bone cements. One representative of three trials is shown for each bone cement. Bone cements tested included: Plain, ZM (containing micron particulate ZrO_2), ZN (containing unfunctionalized ZrO_2 nano-particles), ZNFT (containing functionalized ZrO_2 nano-particles), BM (containing micron particulate $BaSO_4$), BN (containing unfunctionalized $BaSO_4$ nano-particles), and BNFT (containing functionalized $BaSO_4$ nano-particles). **A**) All bone cements, **B**) Bone cements containing ZrO_2 particles, and **C**) Bone cements containing $BaSO_4$ particles.

(BM): 9.71E + 06 N/m^2, bone cements with unfunctionalized $BaSO_4$ nanoparticles (BN): 2.36E + 07 N/m^2, bone cements with $BaSO_4$ nanoparticles functionalized with TMS (BNFT): 1.90E + 07 N/m^2, bone cements with ZrO_2 micron particles (ZM): 7.50E + 07 N/m^2, bone cements with unfunctionalized ZrO_2 nanoparticles (ZN): 1.04E + 07 N/m^2, and bone cements with ZrO_2 nanoparticles functionalized with TMS (ZNFT): 2.36E + 07 N/m^2.

Temperature measurements of bone cements during polymerization

Results of the exothermic testing showed no significant differences in temperature for any of the samples of interest to the present study during polymerization (data not shown).

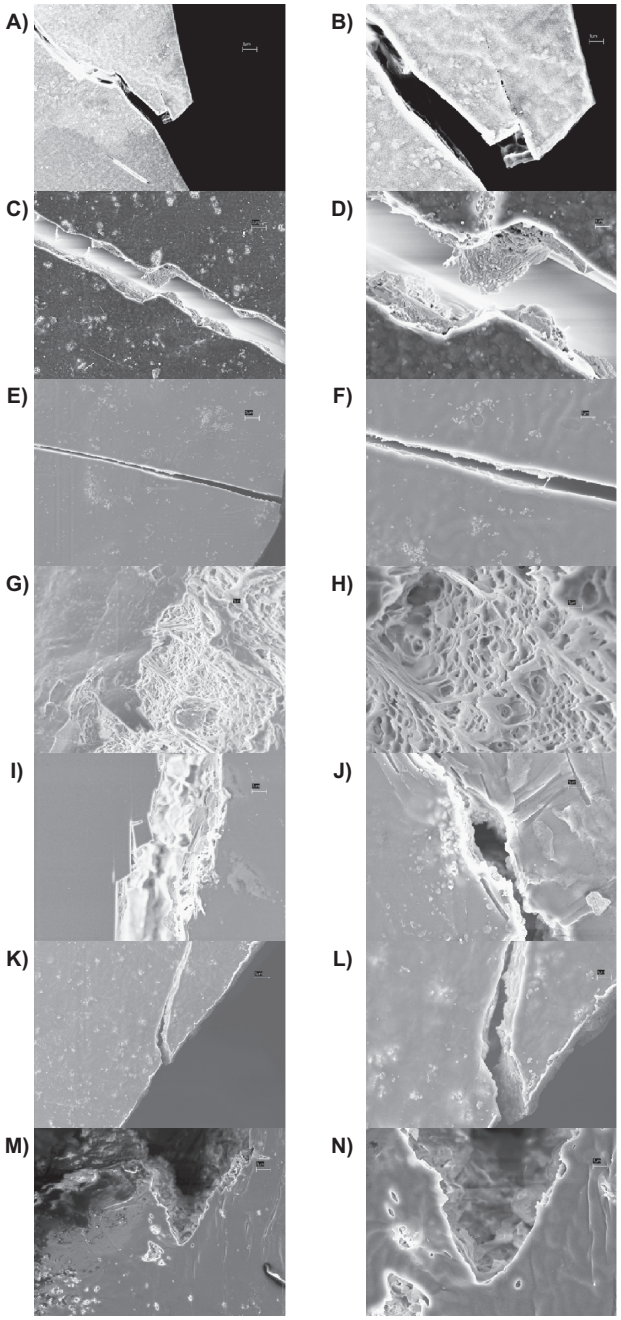

Figure 8 SEM images of bone cements fractured in tension [Left: 5K X (scale bar = 3 μm), Right: 15K X (scale bar = 1 μm)]: Plain (**A, B**), ZM (containing micron particulate ZrO_2) (**C, D**), ZN (containing unfunctionalized ZrO_2 nano-particles) (**E, F**), ZNFT (containing functionalized ZrO_2 nano-particles) (**G, H**), BM (containing micron particulate $BaSO_4$) (**I, J**), BN (containing unfunctionalized $BaSO_4$ nano-particles) (**K, L**), and BNFT (containing functionalized $BaSO_4$ nano-particles) (**M, N**).

X-ray analysis of radio-opacity

Results demonstrated that the radio-opacity of all bone cements with ceramic particles was greater than that of plain bone cements (Table 3).

Table 2 Compressive stress required to obtain 56% strain (1 mm of compression) in various bone cements: Plain, ZM (containing micron particulate ZrO_2), ZN (containing unfunctionalized ZrO_2 nano-particles), ZNFT (containing functionalized ZrO_2 nano-particles), BM (containing micron particulate $BaSO_4$), BN (containing unfunctionalized $BaSO_4$ nano-particles), and BNFT (containing functionalized $BaSO_4$ nano-particles). Maximum compressive stress at 56% strain for bone calculated from Young's moduli values obtained from study by Mente et al

Substrate	Maximum compressive stress (N/m^2)
Plain	–3.63E + 07
BN	–2.36E + 07
ZNFT	–2.36E + 07
BNFT	–1.90E + 07
ZN	–1.04E + 07
BM	–9.71E + 06
ZM	–7.50E + 06
Cortical bone – dry	–1.02E + 10
Cortical bone – wet	–6.94E + 09
Trabecular bone – dry	–4.37E + 09

Table 3 Radio-opacity, as indicated by mean gray value, of various bone cements. Higher mean gray value is indicative of a greater degree of radio-opacity. Bone cements analyzed included: Plain, ZM (containing micron particulate ZrO_2), ZN (containing unfunctionalized ZrO_2 nano-particles), ZNFT (containing functionalized ZrO_2 nano-particles), BM (containing micron particulate $BaSO_4$), BN (containing unfunctionalized $BaSO_4$ nano-particles), and BNFT (containing functionalized $BaSO_4$ nano-particles)

Substrate	Mean gray value (Normalized)
Plain	43.68
ZM	76.59
ZN	76.30
ZNFT	72.66
BM	54.63
BN	49.81
BNFT	63.44

Discussion

Most importantly, cytocompatibility results indicated that the addition of ceramic particles had a positive impact on osteoblast cell density on bone cements. These findings were in agreement with a study carried out by Ricker and colleagues which demonstrated increased osteoblast density on PMMA samples containing ceramic particles, with nanoscaling of certain ceramic particles leading to an even greater increase in osteoblast density (as also demonstrated here).[7] Future experiments need to focus on the mechanisms of why this occurred (most likely due to optimal initial select protein adsorption events important for mediating osteoblast adhesion as noted by others on nanoparticulate polymer composites).[7] In addition, studies to improve the distribution of these nanoceramics in bone cements are needed as other studies have demonstrated improved cytocompatibility properties with fully dispersed nanoparticles in polymers.[7]

In addition, this study provided key information concerning mechanical properties of the bone cements when compared to natural bone. Due to the presence of collagen in bone, plastic deformation regions have been observed which are not currently emulated in traditional bone cements.[7] In the present study, plastic deformation was observed for the bone cements containing nanoparticulates. Further, Mente and colleagues reported that the Young's modulus for different types of bone are: dry cortical bone: 1.82E + 10 N/m^2, wet cortical bone: 1.24E + 10 N/m^2, and dry trabecular bone: 7.80E + 09 N/m^2. In this study, the maximum stress and Young's modulus were found for plain bone cements. Additionally, the Young's moduli of bone cements containing unfunctionalized ZrO_2 micron and nanoparticles were higher on average than the Young's moduli of bone cements containing functionalized ZrO_2 nanoparticles. On average, bone cements containing functionalized $BaSO_4$ nanoparticles had a lower Young's modulus than bone cements containing micron $BaSO_4$ particles, but had a higher Young's modulus relative to bone cements containing unfunctionalized $BaSO_4$ nanoparticles.

Clearly, the stress–strain trends of the bone cements formulated in this study under tensile loading indicated an inherent tradeoff in the mechanical properties. The addition of any ceramic particle was detrimental in that it decreased the maximum tolerable tensile stress as well as the Young's modulus of bone cements. However, as mentioned, the addition of the ceramic nanoparticles functionalized with TMS did, however, have positive implications on the mechanical properties of bone cements as they drastically changed failure modes. The plastic failure mode indicated a potential for aversion of the brittle, and often dramatic, failure that is frequently found with today's bone cements. Future studies will have to optimize the ceramic weight percent addition to PMMA to match the mechanical properties of bone.

Similar promise was observed for the compressive properties of the novel bone cements formulated in this study. Using the Young's moduli found by Mente and colleagues, the maximum compressive stresses corresponding to 56% strain for different types of bone were: dry cortical bone: 1.02E + 10 N/m^2, wet cortical bone: 6.94E + 09 N/m^2, and

dry trabecular bone: 4.37E + 09 N/m^2. In this study, unmodified bone cements had the greatest compressive stress at 56% strain and were most similar to bone. Among bone cements containing ZrO_2 particles, those containing functionalized nanoparticles were the least easily compressed to obtain 56% strain, followed by bone cements containing unfunctionalized nanoparticles, and finally by bone cements containing micron particles. Among bone cements containing $BaSO_4$ particles, those containing unfunctionalized nanoparticles were most easily compressed, followed by bone cements containing functionalized nanoparticles, and finally by bone cements containing micron particles.

In summary, results of the mechanical portion of this study demonstrated a strong ability to tweak mechanical properties of bone cements with nanometer chemically functionally functionalized particles, even achieving plastic deformation regions before failure similar to that of natural bone.

Clearly, one of the largest disadvantages of today's bone cements is that they are largely exothermic, damaging juxtaposed bone and increasing healing time. The exothermic reaction results from this study did, however, deviate from the findings of Ricker and colleagues who demonstrated a markedly decreased temperature change during polymerization of bone cements containing ceramic nanoparticles compared to bone cements containing no ceramic particles or those containing micron ceramic particles.[7] One plausible explanation for the variation observed here compared to such previous studies could be that different ceramic weight percentages were used in this study; such deviation needs to be the focus of future studies.

Lastly, bone cements needs to be radio-opaque in order for proper clinical analysis of bone growth next to bone cements. The radio-opacity experimental results from this study were in agreement with the work of Ricker and colleagues who demonstrated greater radio-opacity with nanometer particles compared to micron particle-doped bone cements.[7] Moreover, here it was observed that the radio-opacity of bone cements with chemically functionalized ZrO_2 nanoparticles was found to be less than the radio-opacity of bone cements with unfunctionalized ZrO_2 micron- and nanoparticles. In contrast, the radio-opacity of bone cements with functionalized $BaSO_4$ nanoparticles was found to be even greater than the radio-opacity of bone cements with unfunctionalized $BaSO_4$ micron- and nanoparticles. Finally, it was also found that bone cements containing ZrO_2 were more radio-opaque than those containing $BaSO_4$ for all particle types: micron, nano, and nanofunctionalized. While all ceramic particles significantly increased the radio-opacity of bone cements, the results indicated that ZrO_2 was relatively better than $BaSO_4$ at doing so.

Conclusions

Recent research in biomaterials has focused on improving biocompatibility properties. Understanding the interaction of biomaterials with tissue *in situ* is of paramount importance towards improving their function and integration into the body.[11] Research has shown that PMMA often elicits an auto-immune response within the body, which may lead to fibrous encapsulation and other physiological responses that destabilize and decrease biocompatibility at the bone-implant interface. In an effort to improve properties of bone cement, Atsushi and colleagues functionalized PMMA with TMS and found that compared to unmodified bone cement, this modified bone cement increased osteoconductivity.[12] Recent studies have also determined that PMMA/hydroxyapatite/nanoclay bone cements promoted osteoconductivity and possessed improved mechanical properties (such as the ability to withstand tensile and shear stresses) compared to unmodified PMMA.[13]

A similar effort was used here to improve properties of PMMA, however, it focused more on nanotechnology approaches. ZrO_2 and $BaSO_4$ micronscale, nanoscale, and nanoscale TMS functionalized particles were introduced into bone cements. Bone cements were subsequently examined for their cytocompatibility and mechanical properties. It was shown that these ceramic particles, which are currently used to aid in the diagnosis of bone cement efficacy through X-ray imaging, did indeed increase cytocompatibility properties, alter mechanical failure mode, and increase the radio-opacity of bone cements. There were no significant differences found in the exothermic polymerization temperatures for any of the bone cements formulated here over time. Bone cements containing nanometer ZrO_2 or $BaSO_4$ particles functionalized with TMS showed the most promise for improving cytocompatibility properties and promoting plastic rather than brittle tensile mechanical failure; as such, they should be further studied for improving properties of traditional PMMA for orthopedic applications.

Acknowledgments

This research was funded by NIH grant 1R43AR056156-01, "Novel Acrylic Bone Cement Using Surface Functionalized Nanoparticles." The authors report no conflicts in this work.

References

1. Charnley J. Anchorage of the femoral head prosthesis to the shaft of the femur. *J Bone Joint Surg Br*. 1960;42-B:28–30.
2. Frick C, Dietz A, Merritt K, Umbreit T, Tomazic-Jezic V. Effects of prosthetic materials on the host immune response: Evaluation of polymethyl-methacrylate (PMMA), polyethylene (PE), and polystyrene (PS) particles. *J Long Term Eff Med Implants*. 2006;16:423–433.
3. Sabokbar A, Fujikawa Y, Murray DW, Athanasou NA. Radio-opaque agents in bone cement increase bone resorption. *J Bone Joint Surg Br*. 1997;79:129–134.
4. Frias C, Frazao O, Tavares S, Vieira A, Marques AT, Simoes J. Mechanical characterization of bone cement using fiber Bragg grating sensors. *Mater Des*. 2009;30:1841–1844.
5. Radev B, Kase J, Askew M, Weiner S. Potential for thermal damage to articular cartilage by PMMA reconstruction of a bone cavity following tumor excision: A finite element study. *J Biomech*. 2009;42:1120–1126.
6. Boner V, Kuhn P, Mendel T, Gisep A. Temperature evaluation during PMMA screw augmentation in osteoporotic bone – An *in vitro* study about the risk of thermal necrosis in human femoral heads. *J Biomed Mater Res B Appl Biomater*. 2009;90:842–848.
7. Ricker A, Liu-Snyder P, Webster TJ. The influence of nano MgO and $BaSO_4$ particle size additives on properties of PMMA bone cement. *Int J Nanomedicine*. 2008;3:125–132.
8. Khang D, Lu J, Yao C, Haberstroh KM, Webster TJ. The role of nanometer and sub-micron surface features on vascular and bone cell adhesion on titanium. *Biomaterials*. 2008;29:970–983.
9. Barrias CC, Martinas MC, Almeida-Porada G, Barbosa MA, Granja PL. The correlation between the adsorption of adhesive proteins and cell behaviour on hydroxyl-methyl mixed self-assembled monolayers. *Biomaterials*. 2009;30:307–316.
10. Mente PL, Lewis JL. Experimental method for the measurement of the elastic modulus of trabecular bone tissue. *J Orthop Res*. 2009;7:456–461.
11. Williams DF. On the mechanisms of biocompatibility. *Biomaterials*. 2008;29:2941–2953.
12. Atsushi S. *In vivo* response of bioactive PMMA-based bone cement modified with alkoxysilane and calcium acetate. *J Biomater Appl*. 2008;23:213–228.
13. Wang CX, Tong J. Interfacial strength of novel PMMA/HA/nanoclay bone cement. *Biomed Mater Eng*. 2008;18:367–375.